Molecular Weight Evolution in the Catalytic Chain Transfer Polymerization of CO_2-Expanded Methyl Methacrylate

Grzegorz Zwolak and Frank P. Lucien*

School of Chemical Sciences and Engineering, The University of New South Wales, UNSW Sydney, NSW 2052, Australia.

Received January 11, 2008; Revised Manuscript Received May 21, 2008

ABSTRACT: Molecular weight evolution in catalytic chain transfer polymerization of methyl methacrylate expanded with dense CO_2 is reported. Experimental molecular weight and polydispersity index data are presented at 50 °C in the range of conversion from 1 to 25%, and at pressures of 5 and 6 MPa. A cobaloxime complex is used as the chain transfer catalyst. Both molecular weight and polydispersity increase in the range of conversion achieved at conditions below the homogeneous expansion limit. Predici simulations suggest that either irreversible catalyst deactivation or cobalt−carbon bond formation, between the catalyst and the propagating radicals, is the most likely mechanism for the increase in molecular weight with conversion. At conditions above the homogeneous expansion limit, a bimodal molecular weight distribution is observed, indicating two zones of polymerization. These conditions produce relatively high molecular weight macromonomers with broad molecular weight distributions.

Introduction

Catalytic chain transfer (CCT) polymerization is one of the most useful techniques for producing low molecular weight macromonomers.[1,2] The catalyst of choice, usually a low-spin Co(II) complex, catalyzes the chain transfer to monomer reaction so efficiently that it produces very low molecular weight polymer with concentrations of the catalyst in the order of 10^{-6} M. In the case of methacrylates, the resulting polymer possesses a terminal double bond that enables it to undergo copolymerization to form more complex structures (block, branched, and star polymers) and xerogel materials.[3−7]

The most widely accepted mechanism for CCT polymerization of methacrylates consists of the following steps (eqs 1-2).

$$R_n^{\bullet} + \text{Co(II)} \xrightarrow{k_{tr}} P_n + \text{Co(III)}-\text{H} \quad (1)$$

$$\text{Co(III)}-\text{H} + M \xrightarrow{k_{fast}} \text{Co(II)} + R_1^{\bullet} \quad (2)$$

This mechanism has evolved from numerous studies focused on low-conversion polymerizations.[7] In the first step, the Co(II) catalyst abstracts a hydrogen atom from the growing polymer radical, leading to termination and the Co(III) hydride species. This reaction is thought to be the rate-determining step. In the second step, Co(III)−H reacts with the monomer, initiating a new growing chain and regenerating the catalyst. The standard method for evaluating the rate coefficient in eq 1 is via the Mayo equation (eq 3).

$$\frac{1}{DP_n} = \frac{1}{DP_{n,0}} + \frac{k_{tr}}{k_p}\frac{[\text{Co(II)}]}{[\text{monomer}]} \quad (3)$$

where DP_n is the number-average degree of polymerization, $DP_{n,0}$ is the number-average degree of polymerization in the absence of the chain transfer catalyst, and k_p is the propagation rate coefficient.

In CCT polymerization of styrenes and acrylates, the propagating radicals form covalent bonds with the catalyst to yield an organometallic species (eq 4).

$$R_n^{\bullet} + \text{Co(II)} \leftrightarrow R_n-\text{Co(III)} \quad (4)$$

This effect lowers the concentration of free catalyst and leads to a large reduction in the measured chain transfer constant (k_{tr}/k_p). The reaction is reversible for styrenic radicals. In the case of acrylates, the cobalt−carbon (Co−C) bonds are so strong that the catalyst is permanently attached to a growing polymer chain, effectively stopping chain transfer to monomer. It has been reported in the literature that Co−C bonds can be cleaved by UV radiation, increasing the chain transfer constant for styrenes,[8] and resulting in living polymerization behavior for acrylates.[9] Co−C bonds involving methacrylates are hindered by steric effects due to the α-methyl group, and are considered to have negligible effect on the chain transfer process.[7]

For practical and economic reasons, polymerization processes have to be taken to high conversions. They are usually conducted in an organic solvent to counter the effects of increasing viscosity. In contrast to low-conversion studies, there have been relatively few kinetic studies on CCT polymerization up to high conversions. A summary of previous work on the high-conversion CCT polymerization of methyl methacrylate (MMA) is given in Table 1. According to the Mayo equation, the molecular weight of the resulting polymer should decrease with increasing monomer conversion. However, to date, only one study on CCT polymerization of MMA has produced results that are consistent with this trend.[12] It is also evident from Table 1 that there is a lack of consistency between the various studies. The molecular weight may be invariant[11] or it may increase with conversion.[10,13]

Previously, we reported CCT polymerization of CO_2-expanded methacrylates and styrene using a cobaloxime catalyst.[15,16] The chain transfer constants were significantly higher than those obtained in the bulk monomers, even in the presence of Co−C bond formation in the case of styrene. This effect was mainly attributed to an enhancement of the chain transfer rate coefficient, arising from a reduction in the viscosity of the medium and therefore implying a diffusion-controlled mechanism. Coupling of CCT with a CO_2-expanded monomer therefore offers greater scope for molecular weight reduction and the ability to tune the molecular weight of the polymer through adjustment of the system pressure.

In this paper, we continue this work and focus on molecular weight evolution during CCT polymerization of CO_2-expanded

* Corresponding author. Telephone: +61-2-9385-4302. Fax: +61-2-9385-5966. E-mail: f.lucien@unsw.edu.au.

10.1021/ma8000737 CCC: $40.75
Published on Web 06/25/2008

Table 1. Summary of Molecular Weight Evolution Data from Studies on the Catalytic Chain Transfer Polymerization of Methyl Methacrylate up to High Conversion

ref	catalyst[a]	solvent, T (°C)	molecular weight evolution
10	COBF	75% toluene, 60	increase in molecular weight over the range of conversion
11	COPhBF	67% toluene, 60	essentially constant molecular weight and polydispersity index
12	COBF[b]	75% toluene, 60	decrease in molecular weight consistent with Mayo equation
13	$Co^{II}TPP$	benzene (2 M MMA), 60	increase in molecular weight
14	COBF	0−83% toluene, 60	decrease in molecular weight smaller than that predicted by Mayo equation

[a] Key: COBF = bis[(difluoroboryl)dimethylglyoximato]cobalt(II); COPhBF = bis[(difluoroboryl)diphenylglyoximato]cobalt(II); $Co^{II}TPP$ = cobalt(II) tetraphenylporphyrin. [b] Co(III) derivative of COBF.

MMA. The experimental section consists of two main parts. In the first part, we consider the volumetric expansion behavior of polymer/monomer mixtures in the presence of dense CO_2. In the second part, we examine the evolution of molecular weight distributions of polymer synthesized in CO_2-expanded MMA. We also present Predici simulations of the CCT model modified with additional reaction steps to explain the experimental results.

Experimental Section

Materials. Methyl methacrylate (99%) was purchased from Sigma-Aldrich and passed through a column of activated basic alumina to remove the polymerization inhibitor (4-methoxyphenol). Liquid CO_2 (99.995%) was obtained from Linde Gases. The polymerization initiator, 2,2′-azobis(isobutyronitrile) (AIBN), was sourced from Dupont and purified by recrystallizing twice from methanol. The chain transfer catalyst, bis[(difluoroboryl)diphenylglyoximato]cobalt(II) (COPhBF, **1**), was prepared according to the procedure described by Bakac et al.,[17] using diphenylglyoxime instead of dimethylglyoxime in the given procedure. The same batch of COPhBF was used in all experiments.

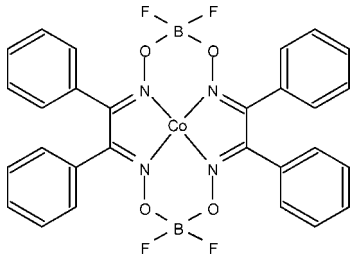

1

Polymerization Procedure. The CCT polymerization of CO_2-expanded MMA was carried out in a 300 mL stirred autoclave reactor. A detailed description of the actual reactor setup is given elsewhere.[15] The reactor was cooled to 5 °C prior to the addition of any materials. An amount of 100 mg of AIBN was added to the reactor followed by the addition of a known volume of monomer. The reactor was sealed and stirring was initiated to mix the AIBN and MMA. The reactor contents were purged with high-purity CO_2 (0.1 MPa) to remove oxygen. A known volume of a catalyst stock solution (1.3×10^{-4} g COPhBF/g MMA) was then added to the reactor. The combined volume of monomer and catalyst solution was kept constant at 100 mL. After catalyst addition, the reactor contents were further purged with CO_2 (0.1 MPa), followed by pressurization with CO_2 to an intermediate level of pressure. Continuous stirring at 800 rpm was maintained during this step to ensure equilibrium between the liquid and vapor phases.

The system was then heated to 50 °C, with stirring at 100 rpm, leading to the desired operating pressure of 5 or 6 MPa (~ 10 min). The catalyst concentration in the expanded solution was maintained constant for all reaction runs at a given operating pressure (see Table 2). In preliminary work, it was established that negligible polymerization of the monomer occurred during this heating stage. The time of the actual polymerization was varied between 1 and 16 h. The conversion of the monomer varied from 1 − 25% on a mass basis, depending on the operating pressure and time of polymerization. This was followed by cooling of the reactor to ambient temperature and subsequent depressurisation to terminate the polymerization. A sample of the partially reacted monomer was collected and evaporated in the presence of hydroquinone to isolate the polymer. The molecular weight distribution of the polymer was determined with size exclusion chromatography. Conversion was determined gravimetrically.

Table 2. Reaction Conditions Used in the Catalytic Chain Transfer Polymerization of CO_2-Expanded Methyl Methacrylate at 50 °C

time (h)	conversion[a] (%)	M_w[b]	M_n[c]	PDI[d]	HEL[e] (MPa)
	$P = 5$ MPa, [catalyst] $= 9.5 \times 10^{-7}$ M				
1	1.8	10500	5340	2.0	>5.4
2	3.1	12800	6460	2.0	>5.4
4	6.1	19100	8780	2.2	>5.4
7	10.7	24200	11000	2.2	5.4
16	25.0	37500	15000	2.5	5.3
	$P = 6$ MPa, [catalyst] $= 7.9 \times 10^{-7}$ M				
1	1.2	9440	4760	2.0	6.1
4	3.0	28900	7350	3.9	5.1
16	10.6	48300	12200	4.0	5.1

[a] The conversion and molecular weight data in the table represent the mean values of at least two experiments. The relative standard deviation with respect to conversion is less than 10%. [b] Weight-average molecular weight. [c] Number-average molecular weight. [d] Polydispersity index. [e] Homogeneous expansion limit.

In an actual polymerization run, the following quantities of materials were combined: 99.7 mg AIBN, 93.9 g MMA and 0.10 mg COPhBF. The liquid phase was expanded with CO_2 up to a pressure of 4.96 MPa at 50 °C. The mixture was polymerized for precisely 1 h resulting in a monomer conversion of 1.9%. The number-average and weight average molecular weights of the polymer were 5110 and 10300, respectively.

Expansion Measurements. Volumetric expansion of monomer/polymer mixtures with CO_2 was examined by direct observation in a high pressure sight gauge. A detailed description of the apparatus and procedure used to measure the extent of volumetric expansion was reported in an earlier study on vapor−liquid equilibria for the CO_2-MMA binary system.[18] At the completion of a polymerization experiment, a sample of the partially reacted monomer was taken from the reactor and introduced into the sight gauge. The glass face of the sight gauge was fitted with a ruler (1-mm graduations) to determine the level of the liquid phase. The volume of liquid corresponding to a given level of liquid in the sight gauge was determined by calibration with ethanol at atmospheric pressure. The mixture was then expanded with CO_2 up to the desired pressure. Recirculation of the liquid phase was maintained until the liquid level stabilized. The volumetric expansion of the liquid phase (E) at a given temperature (T) and pressure (P) was calculated according to the following equation:

$$E(T,P) = \frac{V_L(T,P) - V_L^*(T)}{V_L^*(T)} \times 100\% \qquad (5)$$

where V_L is the volume of the expanded liquid phase and V_L^* is the initial volume of the liquid phase saturated with CO_2 at atmospheric pressure.

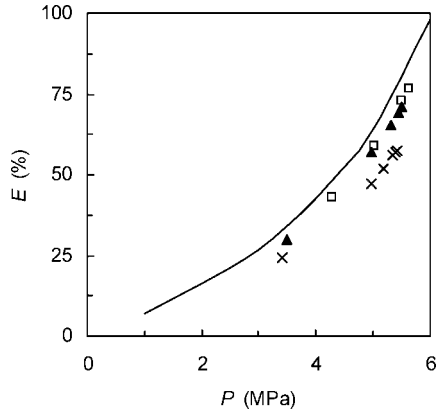

Figure 1. Volumetric expansion (E) of polymer/monomer mixtures with CO_2 as a function of pressure at 50 °C. The solid line represents expansion of polymer-free methyl methacrylate (MMA). The points represent the expansion of various mixtures produced after catalytic chain transfer polymerization of CO_2-expanded MMA at 5 MPa and 50 °C (see Table 2 for conversion and molecular weight data): 4 h (squares), 7 h (triangles), and 16 h (crosses).

Molecular Weight Analysis. Molecular weight distributions were determined by size exclusion chromatography using a Shimadzu LC-10 AT VP pump, a Shimadzu SIL-10AD VP Autoinjector, a column set consisting of a Polymer Laboratories 5.0 μm bead-size guard column (50 × 7.5 mm) followed by three linear PL columns (10^5, 10^4, and 10^3 Å) in a column oven at 40 °C, and a Shimadzu RID-10A differential refractive index detector. Tetrahydrofuran (Ajax, HPLC grade) was used as eluent at 1.0 mL/min. Calibration of the equipment was performed with narrow PMMA standards (Polymer Laboratories), with molecular weights (M_p) in the range 1440 to 1.56 × 10^6 g/mol.

Simulations. Simulation of molecular weight distributions were carried out on a 2-GHz Pentium 4 computer with Windows XP operating system (256 MB RAM). The Predici simulation software (Version 5.36.5) was provided by CiT GmbH (Rastede, Germany).

Results and Discussion

Volumetric Expansion. Volumetric expansion data for various polymer/monomer mixtures synthesized in CO_2-expanded MMA at 5 MPa are shown in Figure 1. The reaction conditions at which these mixtures were produced are listed in Table 2. Liquid volume increases exponentially with pressure, with small amounts (<5%) of low molecular weight polymer causing negligible deviation from the pure monomer expansion line. However, solutions polymerized to higher conversions display a noticeable reduction in the level of expansion. For example, pure MMA expands by 64% when contacted with CO_2 at 5 MPa. The corresponding expansion for a solution polymerized for 16 h is lower by a factor of 0.75. Since the conversion of monomer in the latter is around 25%, it may be concluded that the polymer displaces CO_2 from the liquid phase. This was also observed experimentally by small pressure increases during polymerization. However, this change does not influence the solubility of CO_2 in the monomer to a great extent.

The expansion process leads to the well-known antisolvent effect in which the precipitation of a solute can be induced once a sufficient concentration of CO_2 is attained in the solvent.[19,20] Precipitation of polymer from an expanded polymer/monomer mixture is usually preceded by phase separation. This condition is characterized by a cloudy appearance (emulsion) in the mixture and represents the formation of two immiscible liquid phases. The operating pressure at which phase separation occurs marks the homogeneous expansion limit (HEL) of the mixture. In this study, expansion of the polymer/monomer mixtures was continued until the HEL was reached. It can be seen in Table 2 that the HEL pressure decreases with increasing polymer molecular weight and monomer conversion. The runs performed at an initial pressure of 5 MPa were all under the HEL. Polymerizations conducted at an initial pressure of 6 MPa, however, were above the HEL after 1 h.

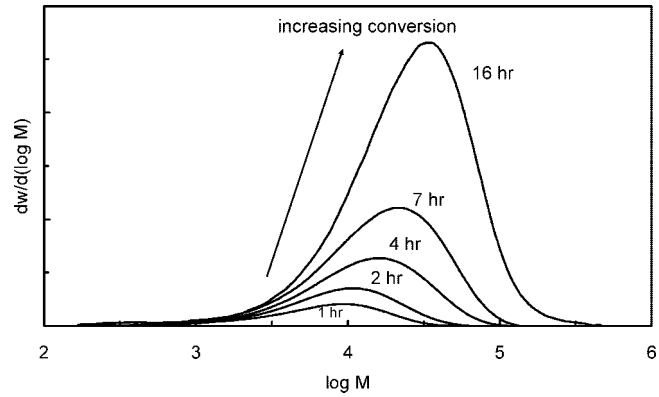

Figure 2. Evolution of molecular weight distributions for polymer produced under the homogeneous expansion limit (P = 5 MPa). Areas under the curves correspond to the conversions.

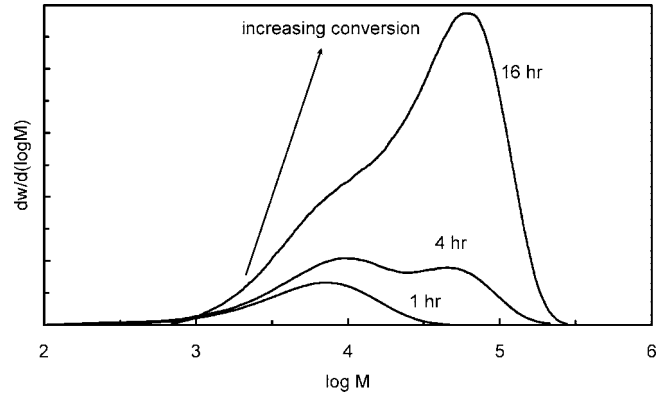

Figure 3. Evolution of molecular weight distributions for polymer produced above the homogeneous expansion limit (P = 6 MPa). Areas under the curves correspond to the conversions.

Molecular Weight Evolution at Conditions below the HEL. The evolution of molecular weight distributions for polymer produced below the HEL is presented in Figure 2. It can be seen that the molecular weight of the polymer increases steadily with conversion, while PDI increases from 2.0 to 2.5 (see Table 2). Specifically, M_w increases by a factor of 3.5 in the range of conversion from 2 to 25%. The increase in molecular weight observed here is much more significant than the examples given in Table 2. Kukulj and Davis[10] reported an increase of around 40% in the range of conversion from 10 to 80%. The PDI also increased slightly from 1.8 to 2.0. They proposed catalyst deactivation by the solvent (toluene) as an explanation for their results. Li and Wayland[13] reported similar increases in molecular weight in the range of conversion from 10 to 50% using cobalt(II) tetraphenylporphyrin in benzene (no PDI data provided). They attributed this result to reinitiation of the terminated polymer by the Co(III) hydride.

Molecular Weight Evolution at Conditions above the HEL. The evolution of molecular weight distributions for polymer produced above the HEL is presented in Figure 3. Polymerization at this pressure (6 MPa) occurs below the HEL only for the first hour (see Table 2). Polymer synthesized in the first hour has the molecular weight distribution of a typical CCT polymer: a single peak of low molecular weight with a PDI of 2. The situation changes dramatically once the system exceeds the HEL at higher conversions. After 4 h, the conversion

reaches 3% and the polymer displays a double-peak distribution with a much higher M_w and a PDI of 3.9. The double-peak distribution indicates two zones of polymerization due to the formation of two immiscible liquid phases, as confirmed by the expansion measurements on this polymer/monomer mixture. Typically, the immiscible phases consist of a CO_2-rich phase and a polymer-rich phase.[20] Since a substantial amount of monomer is present in each phase, we can expect that the catalyst is present in both phases but not necessarily at the same concentration.

In our earlier studies, we demonstrated that the presence of CO_2 enhances molecular weight reduction in CCT by lowering the viscosity of the monomer.[15,16] The lower molecular weight portion of the double-peak distribution can therefore be attributed to the CO_2-rich liquid phase. Conditions in the polymer-rich phase are exactly the opposite. The relatively high viscosity resulting from a reduced CO_2 content retards the termination and chain transfer reactions. This leads to the higher molecular weight portion of the double-peak distribution.

After 16 h of polymerization, there is a shift toward even higher molecular weights in the polymer-rich phase. We can also see that this portion of the distribution is much more pronounced than its lower molecular weight counterpart. This suggests that the rate of polymerization is faster in the polymer-rich phase, a feature once again attributed to a slower termination rate. On the basis of these observations it is clear that it is undesirable to conduct CCT polymerization above the HEL. This aspect will not be considered further in the kinetic modeling section.

Kinetic Modeling. Predici is a simulation package for the kinetic modeling of polyreactions and computation of molecular weight distributions generated in polymerizations. Predici was used to examine the effect of additional steps in the CCT mechanism. Pierik and van Herk[14] have performed Predici simulations to account for higher than expected molecular weights observed during the high conversion solution polymerization of MMA. In general, the kinetic models considered in their study fall under the following categories: irreversible catalyst deactivation via spontaneous decomposition or reaction with impurities (model I); macromonomer reinitiation (model II); reversible catalyst deactivation via Co−C bond formation (model III). In this section, all three of these models are evaluated.

The CCT process shown in eqs 1 and 2 was implemented in the simulation package, along with the following free-radical polymerization steps (eqs 6-9).

$$\mathrm{AIBN} \xrightarrow{k_d} \mathrm{I}_1^{\bullet} + \mathrm{I}_1^{\bullet} \tag{6}$$

$$\mathrm{I}_1^{\bullet} + \mathrm{MMA} \xrightarrow{k_i} \mathrm{R}_1^{\bullet} \tag{7}$$

$$\mathrm{R}_n^{\bullet} + \mathrm{MMA} \xrightarrow{k_p} \mathrm{R}_{n+1}^{\bullet} \tag{8}$$

$$\mathrm{R}_n^{\bullet} + \mathrm{R}_m^{\bullet} \xrightarrow{k_t} \mathrm{P}_n + \mathrm{P}_m \tag{9}$$

The additional equations describing irreversible catalyst deactivation and macromonomer reinitiation by Co(III)−H in models I and II, respectively, are as follows (eqs 10 and 11).

$$\mathrm{Co(II)} \xrightarrow{k_{decom}} \mathrm{Co(II)_{inactive}} \tag{10}$$

$$\mathrm{P}_n + \mathrm{Co(III)}-\mathrm{H} \xrightarrow{k_{fast2}} \mathrm{R}_n^{\bullet} + \mathrm{Co(II)} \tag{11}$$

Reversible catalyst deactivation in model III was accounted for using the following steps (eqs 12 and 13).

$$\mathrm{R}_n^{\bullet} + \mathrm{Co(II)} \xrightarrow{k_{CoC}} \mathrm{R}_n-\mathrm{Co(III)} \tag{12}$$

$$\mathrm{R}_n-\mathrm{Co(III)} \xrightarrow{k_{CoC^{-1}}} \mathrm{R}_n^{\bullet} + \mathrm{Co(II)} \tag{13}$$

The rate coefficients for eqs 2 and 6–9 are given in Table 3. The reaction between MMA and the Co(III) hydride is considered to be nonrate-determining. The rate coefficient for this step (k_{fast}) exceeds the chain transfer rate coefficient (k_{tr}) by orders of magnitude.[12] Typical values of k_{tr} for CO_2-expanded methacrylates vary in the range 10^7-10^8 L mol^{-1} s^{-1}.[15,16] Accordingly, the value of k_{fast} was set to 1×10^9 L mol^{-1} s^{-1} for all three models. The rate coefficient for the decomposition of AIBN in MMA (k_d) was taken from the literature[21] and assumed to be unaffected by the presence of CO_2. Qin et al.[22] have examined the effect of conversion on the initiator efficiency (f) in the bulk free-radical polymerization of MMA. Generally, f is independent of temperature and initiator concentration but decreases markedly at high conversion. The recommended value for f is 0.54 in the low conversion range (<30% at 50 °C). The rate coefficient for initiation (k_i) is not directly required in the simulations, since this step is assumed to be much faster than propagation. The rate coefficient for propagation (k_p) was calculated from a correlation proposed by an IUPAC working party for bulk polymerization of MMA.[23] Beuermann et al.[24] have shown that k_p for MMA in dense CO_2 decreases by around 40% at a pressure of 100 MPa. This effect was assumed to be negligible at 5 MPa.

The value for the average termination rate coefficient (k_t) was obtained from the first order rate plot shown in Figure 4. The initial ($[M]_0$) and final monomer concentrations ($[M]_f$) were calculated from the experimental conversion data (Table 2). The volumetric expansion of the liquid phase, at different conversions, was taken into account in the calculation of the concentration terms. The rate plot exhibits reasonably good linearity and from the slope of the line of best fit, a value for the total radical concentration can be obtained ($[R] = \text{slope}/k_p$). Invoking the steady-state approximation for the total radical concentration leads to the following expression for k_t (eq 14).

$$k_t = \frac{f k_d [\mathrm{AIBN}]}{[\mathrm{R}]^2} \tag{14}$$

From our earlier studies, it was observed that the chain transfer rate coefficient for CO_2-expanded methacrylates and

Table 3. Rate Coefficients Used in Predici Simulations of the Catalytic Chain Transfer Polymerization of CO_2-Expanded Methyl Methacrylate at 50 °C

eq	rate coefficient	value[a]
2	k_{fast}	1×10^9 L mol^{-1} s^{-1}
6	k_d, f	9.7×10^{-7} s^{-1}, 0.54
7	k_i	$k_i > k_p$
8	k_p	649 L mol^{-1} s^{-1}
9	k_t	8.6×10^7 L mol^{-1} s^{-1}

[a] The value for k_{fast} is estimated on the basis that $k_{fast} > k_{tr}$. k_d and f obtained from the literature.[21,22] A value for k_i is not required in Predici simulations under the assumption that $k_i > k_p$. k_p calculated from an IUPAC correlation.[23] k_t calculated using eq 14 and with the total radical concentration derived from Figure 4.

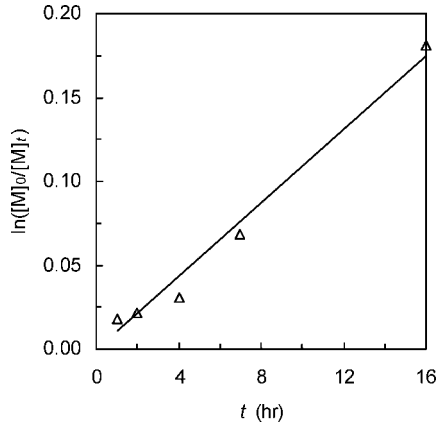

Figure 4. First order rate plot for catalytic chain transfer polymerization of CO_2-expanded methyl methacrylate at 5 MPa and 50 °C.

Table 4. Optimized Rate Coefficients from Predici Simulations

model	k_{tr} (L mol^{-1} s^{-1})	k_{decom} (s^{-1})	k_{fast2} (L mol^{-1} s^{-1})	k_{CoC} (L mol^{-1} s^{-1})	k_{CoC}^{-1} (s^{-1})
I	6.6×10^7	4.6×10^{-5}			
II	1.2×10^8		6.3×10^{12}		
III	8.5×10^7			1.7×10^4	2.0×10^{-5}

styrene increased by a factor of approximately 3 at 50 °C and for an expansion pressure of 5 MPa. Since termination is known to be diffusion-controlled, we would also expect k_t to increase by a similar factor. From the literature, we obtain a value of 2.6×10^7 L mol^{-1} s^{-1} for k_t in MMA at 50 °C and ambient pressure.[21] From Table 3, it can be seen that the value derived from the first order rate plot is larger than the normal value by a factor of 3.

The rate coefficients for eqs 10–13 were unavailable for CO_2-expanded MMA and treated as adjustable parameters during the simulations. The chain transfer rate coefficient (eq 1) was also treated in the same way, even though we have previously determined its value in CO_2-expanded MMA. Cobaloxime catalysts such as COPhBF are prone to deactivation in the presence of small amounts of oxygen. Consequently, the activity of the synthesized catalyst varies from batch to batch and is affected by the duration of time the catalyst is kept in storage. Not surprisingly, reported values of the chain transfer constant for COPhBF in MMA (ambient pressure) vary over a reasonably wide range of 18 000−30 000.[11,15,25,26] Moreover, the experimentally determined chain transfer constants are apparent values obtained from low conversion experiments. Reactive events that lead to an increase in molecular weight, such as those outlined in models I to III, lead to apparent chain transfer constants that are smaller than the true value. Thus, to obtain a satisfactory simulation of the molecular weight data, it is prudent to use k_{tr} as an adjustable parameter.

Optimized values for the adjustable rate coefficients were fitted from the combined set of experimental M_w and M_n data using Predici and are shown in Table 4. The optimal set of rate coefficients for a given model was obtained by minimizing an objective function incorporating the deviations between the calculated and experimental molecular weight data. All simulations were performed in the moments mode and the accuracy was set to 0.01. All concentrations were corrected for expansion of the liquid phase in the presence of CO_2.

Simulation results for model I (irreversible catalyst deactivation) are presented in Figure 5. Overall, this model provides a reasonably good fit of both the M_w and M_n data. The PDI is also well represented by the model (2.0−2.9). The optimized value for k_{tr} (Table 4) is in close agreement with the experimentally determined value of 4.6×10^7 L mol^{-1} s^{-1} from our

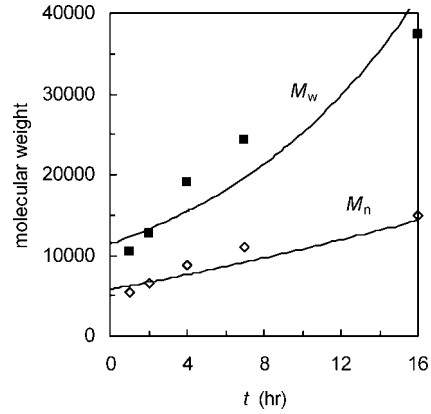

Figure 5. Simulation of molecular weight as a function of time using model I (irreversible catalyst deactivation). Points represent experimental data obtained at 5 MPa (below the homogeneous expansion limit).

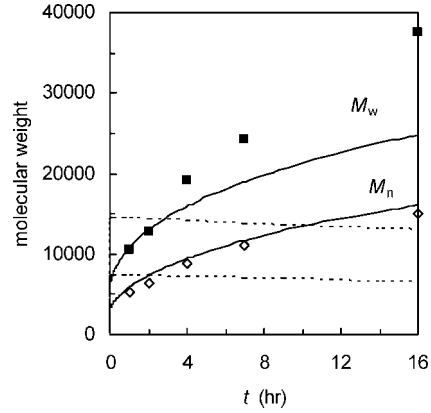

Figure 6. Simulation of molecular weight as a function of time using model II (macromonomer reinitiation). Points represent experimental data obtained at 5 MPa (below homogeneous expansion limit). Solid lines: $k_{fast2} > k_{fast}$. Dashed lines: $k_{fast2} = k_{fast}$.

earlier work.[15] Pierik and van Herk[14] have also considered a first order decomposition model to simulate molecular weight evolution in CCT polymerization of MMA. Although the reaction conditions employed by these workers differ substantially from the present study, their experimental data are well described using a value of 1×10^{-5} s^{-1} for the decomposition rate coefficient, which is consistent with the value reported in Table 4.

The main deficiency with model I is that it predicts an exponentially increasing M_w, even though the experimental data appear to be leveling out in the range of conversion considered. The precise nature of the mechanism of deactivation is also unclear. The effect of oxygen can probably be discounted in view of the degassing techniques employed for the monomer and catalyst stock solutions. Poisoning from other impurities is also unlikely. The purification techniques used here, as well as the sources and purities of MMA and AIBN, are identical to those reported in other studies in which the effects of catalyst deactivation were not observed.[11,12]

Simulation results for model II (macromonomer reinitiation) are shown in Figure 6. In comparison to model I, the fit of the M_n data is much improved while the trend in the simulated M_w data is more consistent with experimental results. However, the model significantly underestimates M_w, leading to lower than expected values of PDI (1.5−1.8) in the given range of conversion. The fitted value for k_{tr} is slightly higher than expected but still exhibits the correct order of magnitude. In contrast, chain transfer to polymer (k_{fast2}) is several orders of

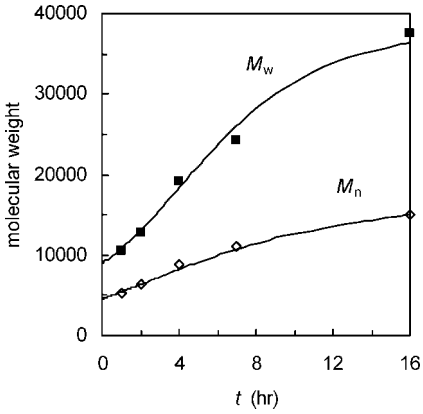

Figure 7. Simulation of molecular weight as a function of time using model III (cobalt−carbon bond formation). Points represent experimental data obtained at 5 MPa (below the homogeneous expansion limit).

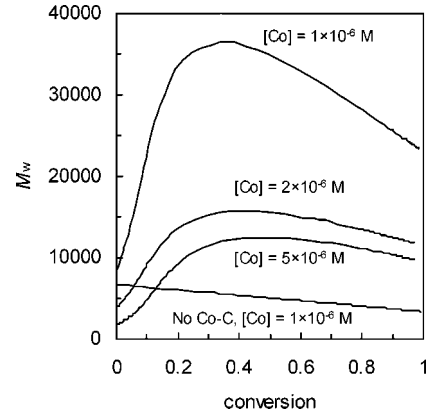

Figure 8. Simulation of molecular weight as a function of conversion using model III (cobalt−carbon bond formation).

magnitude faster than chain transfer to monomer (k_{fast}), which seems physically unlikely. Pierik and van Herk[14] also obtained an improved simulation of M_w data with $k_{fast2} > k_{fast}$, but considered this mechanism to be unlikely. As a further point of interest, simulation results obtained by setting $k_{fast2} = k_{fast}$ are also shown in Figure 6. In this situation, it can be clearly seen that the simulation does not adequately represent the experimental data.

Simulation results for model III (Co−C bond formation) are shown in Figure 7. This model is proposed cautiously because it includes an extra adjustable rate coefficient relative to the other models. An improvement in the simulation is inevitable with a greater number of adjustable parameters. Nonetheless, it can be seen that there is very close agreement between the model and both the M_w and M_n data. The fitted value of k_{tr} is intermediate to the values obtained for the other models.

As noted earlier, Co−C bond formation is very well-known in CCT polymerization of styrenes and acrylates. The extent of the Co−C bond formation is known to be dependent on the type of monomer, solvent and structure of the catalyst, including the type of equatorial and axial ligands.[7] Lewis acid−base interactions between aromatic solvents (base) and the Co(II) species (acid) may compete with the Co−C bond formation reaction represented by eq 12. This may partially explain the apparent absence of Co−C bond formation in solution polymerization of methacrylates, particularly when toluene is used as a solvent. Toluene is known to lower the chain transfer constant of COBF with MMA.[27] Bulky axial ligands in the catalyst structure would also limit Co−C bond formation. For example, the pyridine ligands used by Kowollik and Davis[12] are much more effective in preventing Co−C bonds than the water or methanol ligands used in other studies. Carbon dioxide on the other hand is a weak Lewis acid.[18,28,29] Therefore, its presence in the expanded monomer would not be expected to inhibit Co−C bond formation.

There is, however, no direct evidence of cobalt−carbon bond formation in CCT involving methacrylates. On the basis of experiments conducted in an electron paramagnetic resonance tube (EPR), Heuts et al.[11] concluded that Co−C bonds are absent in CCT polymerization of MMA. EPR spectra have to be recorded under cryogenic temperatures. The solutions prepared by Heuts and co-workers were frozen after only 1 h of polymerization, with the concentration of Co(II) very much larger than the concentration of polymer radicals. It is entirely possible that the extent of Co−C bond formation at such low conversion was too small to be detected by EPR. In the present work, the fitted rate coefficient for eq 12 has a value of 1.7×10^4 L mol^{-1} s^{-1}. This reaction is several orders of magnitude slower than the rate of transfer to monomer, which in turn would make minimal difference to EPR spectra at low conversion.

Due to the reduced solubility of the polymer in the CO_2-expanded monomer, as indicated by the HEL in Table 2, we were unable to continue this experiment beyond 25% conversion. Higher conversions below the HEL could be achieved using higher catalyst concentrations to reduce molecular weight. Alternatively, performing the polymerization in a CO_2-expanded solvent such as toluene would also extend the range of conversion. In this context, the fitted parameters for model III can be used to provide an indication of the likely effect of Co−C bond formation over the whole range of conversion, as shown in Figure 8.

Beginning with the standard CCT model (eqs 1, 2, 6–9), we can see the gradual decrease in M_w with conversion. When Co−C bond formation is incorporated into the model, M_w reaches a maximum value and then decreases in a manner similar to the standard CCT model. The maximum indicates that an equilibrium is reached between eqs 12 and 13, leading to a stable concentration of the uncomplexed Co(II) species. It is interesting to note that the data reported by Kukulj and Davis[10] also exhibit the appearance of a maximum at a conversion of around 70%. The location of the maximum would be expected to depend on the experimental conditions. In Figure 8, for example, a higher initial concentration of catalyst leads to a shift in the maximum M_w to higher conversion. This reflects the greater duration of time required to deplete the catalyst.

Conclusions

Molecular weight evolution in the CCT polymerization of CO_2-expanded MMA is highly dependent on the phase behavior of the reaction system. At conditions above the homogeneous expansion limit, a bimodal molecular weight distribution is observed, indicating two zones of polymerization. These conditions produce relatively high molecular weight macromonomers with broad distributions. Molecular weight increases steadily in the range of conversion achieved at conditions below the HEL but the PDI increases only marginally above a value of 2. Predici simulations suggest that either irreversible catalyst deactivation or Co−C bond formation, is the most likely mechanism for the increase in molecular weight with conversion. The rate coefficient for Co−C bond formation between the catalyst and the propagating radicals is estimated at 10^4 L mol^{-1} s^{-1}, several orders of magnitude below that for chain transfer to monomer. The relatively slow rate of this competing reaction makes its effects noticeable only at higher conversions. This may provide an explanation for the discrepancies that exist between other high-conversion studies.

Acknowledgment. Financial support from the Australian Research Council is gratefully acknowledged.

References and Notes

(1) Burczyk, A. F.; O'Driscoll, K. F.; Rempel, G. L. *J. Polym. Sci., Polym. Chem. Ed.* **1984**, *22*, 3255–3262.
(2) Enikolopyan, N. S.; Smirnov, B. R.; Ponomarev, G. V.; Belgovskii, I. M. *J. Polym. Sci., Polym. Chem. Ed.* **1981**, *19*, 879–889.
(3) Cacioli, P.; Hawthorne, D. G.; Laslett, R. L.; Rizzardo, E.; Soloman, D. H. *J. Macromol. Sci., Chem.* **1986**, *23*, 839–852.
(4) Krstina, J.; Moad, G.; Rizzardo, E.; Winzor, C. L. *Macromolecules* **1995**, *28*, 5381–5385.
(5) Muratore, L. M.; Steinhoff, K.; Davis, T. P. *J. Mater. Chem.* **1999**, *9*, 1687–1691.
(6) Muratore, L. M.; Davis, T. P. *J. Polym. Sci., Part A: Polym. Chem.* **2000**, *38*, 810–817.
(7) Gridnev, A. A.; Ittel, S. D. *Chem. Rev.* **2001**, *101*, 3611–3659.
(8) Pierik, S. C. J.; Vollmerhaus, R.; Van Herk, A. M.; German, A. L. *Macromol. Symp.* **2002**, *182*, 43–52.
(9) Wayland, B. B.; Mukerjee, S.; Poszmik, G.; Woska, D. C.; Basickes, L.; Gridnev, A. A.; Fryd, M.; Ittel, S. D. In *Controlled Radical Polymerization*; Matyjaszewski, K., Ed.; ACS Symposium Series 685; American Chemical Society: Washington, DC, 1998; pp 305−315..
(10) Kukulj, D.; Davis, T. P. *Macromol. Chem. Phys.* **1998**, *199*, 1697–1708.
(11) Heuts, J. P. A.; Forster, D. J.; Davis, T. P.; Yamada, B.; Yamazoe, H.; Azukizawa, M. *Macromolecules* **1999**, *32*, 2511–2519.
(12) Kowollik, C.; Davis, T. P. *J. Polym. Sci., Part A: Polym. Chem.* **2000**, *38*, 3303–3312.
(13) Li, Y.; Wayland, B. B. *Macromol. Rapid Commun.* **2003**, *24*, 307−310.
(14) Pierik, S. C. J.; van Herk, A. M. *J. Appl. Polym. Sci.* **2004**, *91*, 1375–1388.
(15) Zwolak, G.; Jayasinghe, N. S.; Lucien, F. P. *J. Supercrit. Fluids* **2006**, *38*, 420–426.
(16) Zwolak, G.; Lucien, F. P. *Macromolecules* **2006**, *39*, 8669–8673.
(17) Bakac, A.; Brynildson, M. E.; Espenson, J. H. *Inorg. Chem.* **1986**, *25*, 4108–4114.
(18) Zwolak, G.; Lioe, L.; Lucien, F. P. *Ind. Eng. Chem. Res.* **2005**, *44*, 1021–1026.
(19) Xu, Q.; Han, B.; Yan, H. *J. Appl. Polym. Sci.* **2003**, *88*, 2427–2433.
(20) Yeo, S.-D.; Kiran, E. *J. Supercrit. Fluids* **2005**, *34*, 287–308.
(21) *Polymer Handbook*, 4th ed.; Brandrup, J.; Immergut, E. H.; Grulke, E. A., Eds.; John Wiley and Sons: New York, 1999.
(22) Qin, J.; Guo, W.; Zhang, Z. *Polymer* **2002**, *43*, 4859–4867.
(23) Beuermann, S.; Buback, M.; Davis, T. P.; Gilbert, R. G.; Hutchinson, R. A.; Olaj, O. F.; Russell, G. T.; Schweer, J. *Macromol. Chem. Phys.* **1997**, *198*, 1545–1560.
(24) Beuermann, S.; Buback, M.; Schmaltz, C.; Kuchta, F-D. *Macromol. Chem. Phys.* **1998**, *199*, 1209–1216.
(25) Heuts, J. P. A.; Forster, D. J.; Davis, T. P. *Macromolecules* **1999**, *32*, 3907–3912.
(26) Heuts, J. P. A.; Forster, D. J.; Davis, T. P. *Macromol. Rapid Commun.* **1999**, *20*, 299–302.
(27) Suddaby, K. G.; Maloney, D. R.; Haddleton, D. M. *Macromolecules* **1997**, *30*, 702–713.
(28) Kazarian, S. G.; Vincent, M. F.; Bright, F. V.; Liotta, C. L.; Eckert, C. A. *J. Am. Chem. Soc.* **1996**, *118*, 1729–1736.
(29) Zhao, F.; Fujita, S.-I.; Sun, J.; Ikushima, Y.; Arai, M. *Chem. Commun.* **2004**, *20*, 2326–2327.

MA8000737